Energy 248 (2022) 123551

Contents lists available at ScienceDirect

Energy

journal homepage: www.elsevier.com/locate/energy

Simultaneous reduction of NOx emission and SOx emission aided by improved efficiency of a Once-Through Benson Type Coal Boiler

Malebo Mollo [a], Andrei Kolesnikov [a], Seshibe Makgato [b, *]

[a] Department of Chemical, Metallurgical and Materials Engineering, Tshwane University of Technology, Private Bag X680 Pretoria 0001, South Africa
[b] Department of Chemical Engineering, College of Science, Engineering and Technology, University of South Africa (UNISA), C/o Christiaan de Wet & Pioneer Avenue, Florida Campus, 1710, Johannesburg, South Africa

ARTICLE INFO

Article history:
Received 3 August 2021
Received in revised form
7 February 2022
Accepted 20 February 2022
Available online 22 February 2022

Keywords:
Nitrogen oxide
Sulphur dioxide
Once-through boiler
Emissions
Power plants

ABSTRACT

With significant contributions in global emissions of air pollutants, sustainable practices for coal-fired power generation are fundamental to mitigate global climate change, besides ensuring compliance to the local authorities, which is as critical as climate issues. Despite the importance of these issues, some gaps exist in the literature to develop practices capable of fostering emissions reduction of NOx and SOx. In this sense, the present study aimed to present a comprehensive approach to NOx emission and SOx emission reduction through improved efficiency of a once-through Benson type coal boiler in a coal-fired power plant. In improving efficiency, NOx and SOx emissions were strongly influenced by O_2 concentration, coal mass flow, air/fuel ratio and coal calorific value. The optimum conditions that resulted in simultaneous reduction of NOx and SOx emissions were achieved when the O_2 concentration was 3.28 vol% with the coal mass flow of 281 tonnes/hr. The results further suggested that NOx concentration was reduced by a large margin when the air/fuel ratio changed from the lean side to the rich side. The findings of this study help to establish benchmarks relating to a comprehensive assessment of SOx and NOx emissions reduction.

1. Introduction

South Africa rely heavily on coal for its energy requirements. It is anticipated that coal will control the South African energy mix in the long run based on low operational cost and abundance [1]. On the other hand, energy consumption has increased exponentially because of population density, industrialization, urbanization, and modernization [2]. According to Bekker et al. [3], earlier than 1990, less than 33% of the South African population had access to electricity. However, the 1996 census indicated that only 58% of South Africa's citizens had access to electricity, and the percentage had doubled by year 2000 [3]. According to StatsSA [4], electricity access in the Republic of South Africa improved from nearly 35% of homes in 1990 to 84% in 2011. The later rapid expansion of the electricity demand and growing need for more electricity has raised the necessity for integrated energy mix and improved power generation capacity and efficiency of the existing power plants. The energy resource structure of South Africa determines that more than 95% of the electric energy production depends on coal-fired plants. Recently, energy demands coupled with stricter environmental regulations have encouraged the implementing of coal-fired power plants optimization analysis [5]. According to Gu et al. [5], better system performance implies increased power generation and decreased maintenance costs.

Power plants coal combustion process goes along with the production of numerous gaseous pollutants including H_2O, NO_x, CO_2, SO_x and smoke dust [1,6]. Gaseous pollutants are regarded as a major environmental issue worldwide. Compared to other pollutants, nitrogen oxides (NOx), and sulphur oxides (SOx) emissions have drawn attention because they affect monuments due to acid rain and leads to corrosive reactions [1]. According to Gani et al. [7], various health conditions and diseases such as the damaging of many human organs appear to result from short exposure to SO_x and NO_x. Furthermore, SOx are a respiratory irritant thus a range of exposure limits pose risks of asthma, lung cancer and bronchitis [8]. Among these impacts, the emissions from coal-burning not only affect local air quality but also travel long distances and cause regional/global environmental issues. Lately, anthropogenic oxides of nitrogen, oxides of sulphur and oxides of carbon emission from

* Corresponding author.
E-mail address: makgato2001@yahoo.com (S. Makgato).

https://doi.org/10.1016/j.energy.2022.123551
0360-5442/

the coal-fired power plants have provoked increasing focus [9]. Governments in many parts of the world have recognized the problems and have moved towards reducing the amount of NOx and SOx emissions through legislation [10]. Currently, the minimum emissions standards (MES), which are being applied in several countries, have put combustion, metallurgical industries, and gasification coal users under growing pressure to decrease the high emissions level in their operations. In South Africa, it is necessary to comply with the current limit of oxides of nitrogen and oxides of sulphur of 750 mg/Nm^3 and 3500 mg/Nm^3 at 6% O_2 to stabilize the global temperature and reverse the warming situation [11]. According to Zheng et al. [12], stricter limits are to be expected in the future. To comply with strict legislation on NO_x and SOx, actions have been taken to reduce emissions from coal-fired power stations [13].

Some studies have already demonstrated the potential of de-NOx technologies such as selective catalytic reduction, air staging, reburning etc. which have been employed to reduce the emission of NOx [6]. Notwithstanding the achievements of some of these methods in removing produced NOx (up to 90%) with a selective catalytic reduction [14], it is important to reduce the overall NOx production during the combustion process. On the other hand, many NOx reduction techniques generally require prediction values of NOx emission as the reference for the optimization process. Already Zhou et al. [15] introduced a method to forecast the NOx emission characteristics of large capacity pulverized power plants with artificial neural networks. Li and Yao [16] employed the low NOx combustion technology method, built on artificial intelligence to cut down NOx emissions, in which air and fuels are sent into the furnace in different layers. According to Li and Yao [16], artificial intelligence exploits advanced computational intelligence algorithms and operation data or thermal adjustment test data to reduce NOx emission. In summary, there are many technologies to deal with NOx formation, such as low-NOx burner, air distribution, fuel burning, and flue gas recirculation, among which the air distribution is the most broadly applied technology to improve utility boiler's operation performance [17]. Although denitrification devices can reduce NOx emissions to a large extent, costs of investment, operation and maintenance are too high [16].

To mitigate 80% of SOx emissions from coal-fired power generation, attention has been drawn to various technologies such as pre-combustion, during combustion and post-combustion techniques. These techniques for instance include physical removal of sulphur in coal before combustion, using sorbent injection to the boiler to absorb sulphur oxides during combustion and using flue gas desulphurization (FGD) to remove SOx from plant gas emissions after combustion [1]. So far, most of the reported studies on SOx emissions reduction of coal-fired power plants focused on established commercialized techniques such as FGD and sorbent injection. However, these techniques are costly and difficult to retrofit on ageing coal-fired plants. Therefore, despite the importance of these issues, very little has been done on boiler combustion optimization for simultaneous reduction of SOx and NO_X emissions. Based on the literature review, it is evident that some gaps exist on once-through Benson type steam boilers emissions reductions as previous studies focused mainly on the improvement of the combustion process quality and reduction of heat losses [18]. To address this problem, this study hopes to establish benchmarks relating to a comprehensive assessment of SOx and NOx emissions reduction by identifying possible boiler combustion inefficiencies and optimizing them.

2. Materials and methods

2.1. Experimental set-up

The experiment was carried out on a typical 660 MW once-through Benson type steam boiler unit of a coal-fired power station located in South Africa. The unit boiler is equipped with 20 burners arranged in five levels of four. The forced draught fans supply secondary air to the burner wind boxes, while primary air fans supply air to the coal mills to carry the air-fuel mixture to the burners. Two induced draught fans draw the combustion gases from the furnace over the surfaces of the superheaters, reheaters, economizer and air preheaters, then via the electrostatic precipitators for discharge to the chimney. The O_2 concentration was varied between 2.90 vol% and 3.80 vol% by adjusting the setpoint. The O_2 levels are not being maintained above 2.5 vol% as per fossil fuel-fired regulations. Additionally, the total airflow was then varied at approximately 643–656 kg/s. The required amount of coal was homogenized and loaded at 90 kg/s. The arrangement of the inlets and the dimension of the furnace are shown in Fig. 1.

2.2. Coal samples and sample preparation

All studies were conducted on coal samples collected from stockpiles of a power plant as received from Waterberg Coalfield. Coal samples were collected and prepared for different analysis using standard procedures.

2.3. Coal analysis methods

Ultimate analysis such as carbon (C), hydrogen (H) and nitrogen (N) were determined using LECO-932 CHNS Analyser following ISO 12902 [19] standard procedure. Reproducibility for C, H and N are ±0.5%, ±0.25% and ±0.10% respectively [19]. The total sulphur was determined in duplicates using Leco S-628 Elemental analyzer at 1350 °C following ASTM D4239-14 [20] standard procedure. Coal samples were burnt in a bomb calorimeter and the calorific value (CV) was measured following ISO 1928 [21] method. The results of duplicated determinations of these CV values should not differ by more than 0.12 MJ/kg indicating the extent of repeatability. Ash content was measured in a furnace maintained at a temperature of 815 °C ± 10 °C using ISO 1171 [22] standard procedure. In addition, Perkin-Elmer Thermo-Gravimetric analyser (TGA) was used to determine total moisture, ash, volatile matter, and fixed carbon by difference (weight %).

2.4. Petrographic analysis - sample preparation

The samples were received crushed to − 1 mm. The particles were set in epoxy resin under vacuum (24 h) and the block was subsequently ground to achieve a polished surface, as per ISO 7404–2 [23] using a Struers Tegraforce polisher.

2.5. Petrographic analysis - methodology

The polished blocks were assessed using a Zeiss AxioImager M2M petrographic microscope fitted with a Fossil Hilgers system with a semi-automated point counting stage for maceral analysis, at a magnification of × 500 under oil immersion. Coal macerals were determined following the ISO 7404–3 [24] standard procedure. Results are reported on a volume % basis, and all macerals are

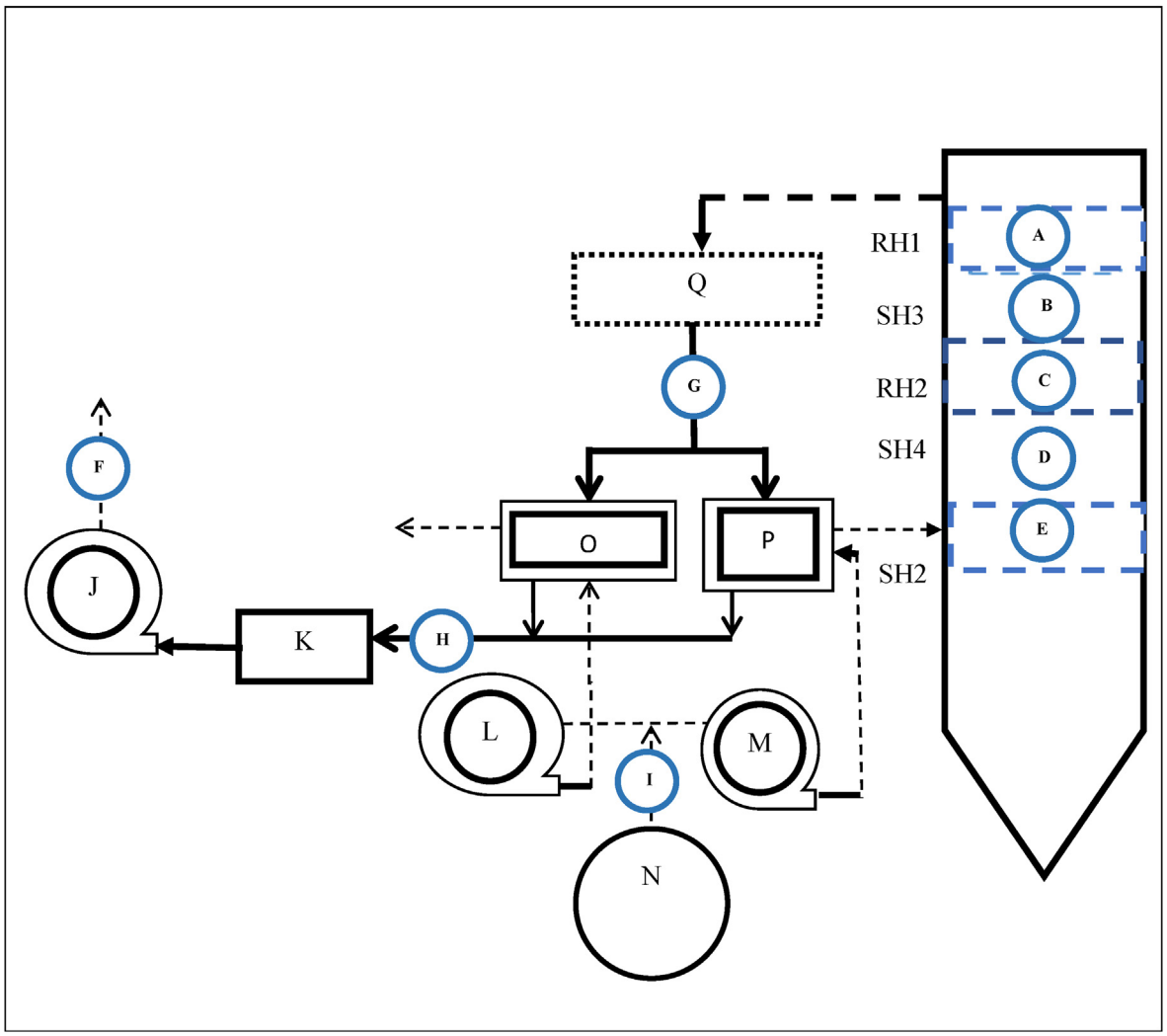

Fig. 1. Plant component layout consisting of A - Reheat 1 (RH1) Temperature & Pressure measurement point, B- Superheater 3 (SH3) Temperature & Pressure measurement point, C - Reheater 2 (RH2) Temperature & Pressure measurement point, D - Superheater 4 (SH4) Temperature & Pressure measurement point, E – Superheater 2 (SH2) Temperature & Pressure measurement point, F - O_2 and SO_2 concentration measurement at the stack, G - O_2 and SO_2 concentration measurement at Economizer outlet point, H - Gas intel temperature measurement point, I - Total airflow measurement point, J - Induced Draft Fan, K - Electrostatic Precipitators, L - Primary Air Fan, M – Forced Air Fan, N- Total Air, O- Primary Air Preheater, P- Secondary Air Preheater, Q- Economizer, R- Boiler.

included in the count.

2.6. Determination of ash oxides

Philips PW2404 X-ray fluorescence (XRF) spectrometer was used to determine the elemental composition of coal ash oxide following the ASTM D3682-13 [25] method.

2.7. Emissions measurement

Exhaust gases were frequently sampled and SO_X and NO_X emissions measured online when power plant was operated in various load conditions using MultiGasAnalyser (Dr Födisch, MGA 23). The calibration of the MGA 23 analyser was performed before the experiments. The acceptable tolerance ranges/values for SO_X and NO_X were not more than 2% of compared reference measurement.

3. Results and discussions

3.1. Petrographic properties

Petrographic properties have been beneficial in assessing feed coal for combustion. Therefore, the interrelationship between coal petrographic properties and steam output, the flame shape and stability, an amount of unburnt carbon and thermographic data and combustion efficiency are key in assessing the performance of coals in combustion processes. The maceral composition, mineral group and reflectance properties used for this study were characterized and the values are presented in Table 1. Little is known regarding the petrographic changes that take place during low-temperature solvent extraction conducted at temperatures below the pyrolysis temperature of coal (generally below 350 °C, depending on the type of coal). Low-temperature solvent extraction can be used to obtain various chemicals and carbon products from coal before combustion [26]. The maceral composition, mineral group and reflectance data are presented in Table 1. The results showed that there are three main coal group macerals of the coal samples studied, viz:

Table 1
Maceral group analysis (% by volume, including mineral matter).

Property	Description	Sample 1	Sample 2	Sample 3	Sample 4	Sample 5
Macerals Group	Vitrinite	20.4	24.4	21.9	22.1	20.3
	Liptinite	1.8	4.3	3.8	2.0	1.9
	Inertinite	34.4	40.9	47.8	42.4	41.3
Mineral Group	Clays	16.3	8.7	5.8	9.3	16.2
	Quartz	19.8	19.7	17.3	18.6	17.9
	Pyrite	2.6	1.2	0.6	1.8	2.4
	Carbonates	2.9	1.4	2.6	2.6	2.9
	Other minerals	1.2	0.4	0.2	0.6	0.4
Rank	R_r	0.71	0.71	0.71	0.71	0.71
	R_m	0.76	0.76	0.76	0.76	0.76

vitrinite, liptinite and inertinite.

The coal samples are dominated by inertinite (Fig. 2) in the range of 34.4–47.8 vol%. Concerning the inertinite assemblage, the macerals determined in coal samples in the current study were in agreement with a study by Wagner et al. [27]. Wagner et al. [27] summarized that Gondwana coals, including those from South Africa, are naturally enriched in inertinite as opposed to the other coal macerals, and semifusinite occurs across a wide range of reflectance. Furthermore, these results appear to be in good agreement with previous work undertaken by Moroeng et al. [28] who reported that South Africa Gondwana coals are naturally enriched in inertinite. The significance of this maceral in the context of combustion is that according to Cloke et al. [29], the inertinite maceral group have often been affiliated with burnout problems.

Fig. 3 provides images of vitrinite observed in the Waterberg coal samples. All five samples have a total vitrinite content in the range of 20.3–24.4 vol%. It is generally accepted that vitrinite formed under quiet, waterlogged conditions where gelification of botanical structures occurred to varying degrees [27]. The vitrinite content in the coal and mudstone decreases with depth in the formation, whereas the concentrations of the inertinite macerals generally increase with depth [30]. Vitrinite has been reported to burn readily, although the rate of burnout decreases as its reflectance increases [31]. Given the intensity of variance exhibited by the major maceral differences in the Grootegeluk Formation, the amount of vitrinite and inertinite macerals and their discrepancy appears to be based on a manifestation of different degrees of maceral group degradation. The possible reason for this variation is tied to changing climatic, tectonic and sedimentary settings with time [27].

Fig. 2 depicts the liptinite macerals (typically formed from spores, pollen, algae, wax coatings of leaves, etc.) observed in these Waterberg coal samples. On an mmf basis, all five samples had minimal liptinite content in the range of 1.8–4.3 vol% which is typical of South African Permian-aged coals [26], which are highly variable and have different trends in the coal and mudstone groups. This observation agrees with the results of Faure et al. [30], who found that liptinite occurs only in minor proportions and is highly variable in the Waterberg coals analyzed. Previous studies by Snyman [31] also observed that South African humic coals are characterized by their low contents (generally less than 5 vol%) of liptinite. Using the Single-Scan method (blue and white light), a far higher proportion of liptinite was determined in all the Waterberg coals samples analyzed by Wagner et al. [27] between 2009 and 2011 to date. The ROM liptinite content ranged from 22 to 34 vol% mmf (or 13.8 to 21.6 vol% inc. mm) in the Waterberg coal samples (which is about 8–12 times processed coal), as determined under blue and white light. Liptinite macerals are derived from hydrogen-rich plants and algal materials [32].

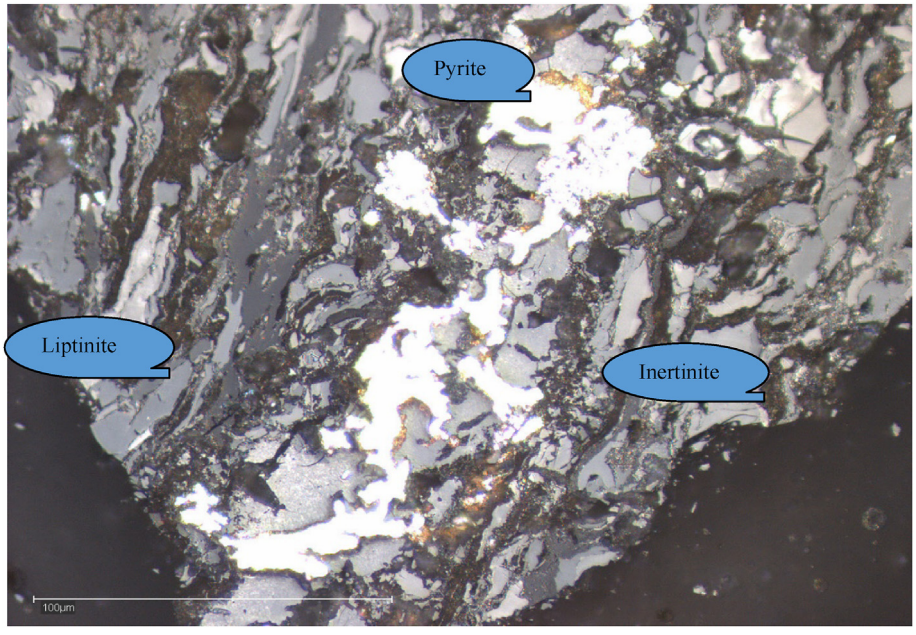

Fig. 2. Micrographs of pyrite, liptinite and inertinite observed in coal samples.

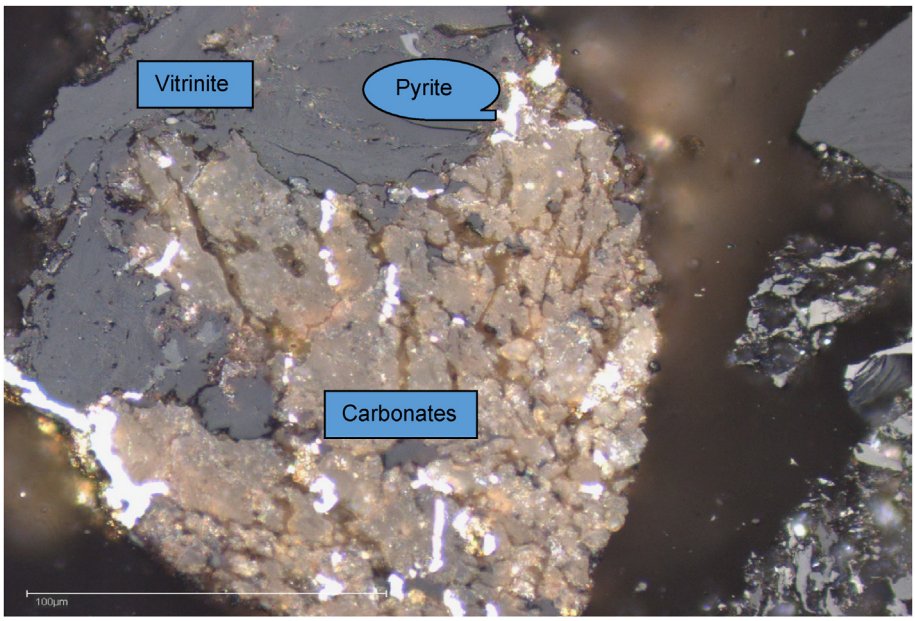

Fig. 3. Micrographs of vitrinite, pyrite and carbonates observed in coal samples.

The petrographically observable mineral matter was separated into silicates (clays of 5.8–16.3 vol% and quartz of 17.3–19.8 vol%) (Fig. 4), sulphides (pyrite of 0.6–2.6 vol% (Fig. 2), carbonate of 1.4–2.9 vol% (Fig. 2) and other minerals of 0.2–1.2 vol% (Fig. 5). The results here were following the study of Wagner et al. [27, who found that minerals observed in all Waterberg coalfield samples were primarily clays (reported as silicates), with some pyrite and carbonate minerals observed. Snyman [31] produced a vast amount of good quality data while studying minerals in South African coals and established that the dominant minerals in South African coals are clays, carbonates, sulphides, quartz and glauconite which support the current study. This interpretation is supported by the work of Faure et al. [30], in which the quartz content of about 19.8% (by vol) was observed. According to Moroeng et al. [28], the average grain size of quartz improves toward the top of the formation, where the grains are silt size on average. All samples contained low levels of pyrite, and pyrite occurred in vitrinite and inertinite macerals, in syngenetic and epigenetic structures. When it comes to Waterberg coal maceral analysis, different results have been seen based on ROM coal, processed coal and coal types.

Coal samples were rated in the high-volatile bituminous range according to a mean maximum reflectance of 0.76% (mean random). This reflectance value was consistent with previously published values for Waterberg coals by Van Niekerk et al. [26]. The

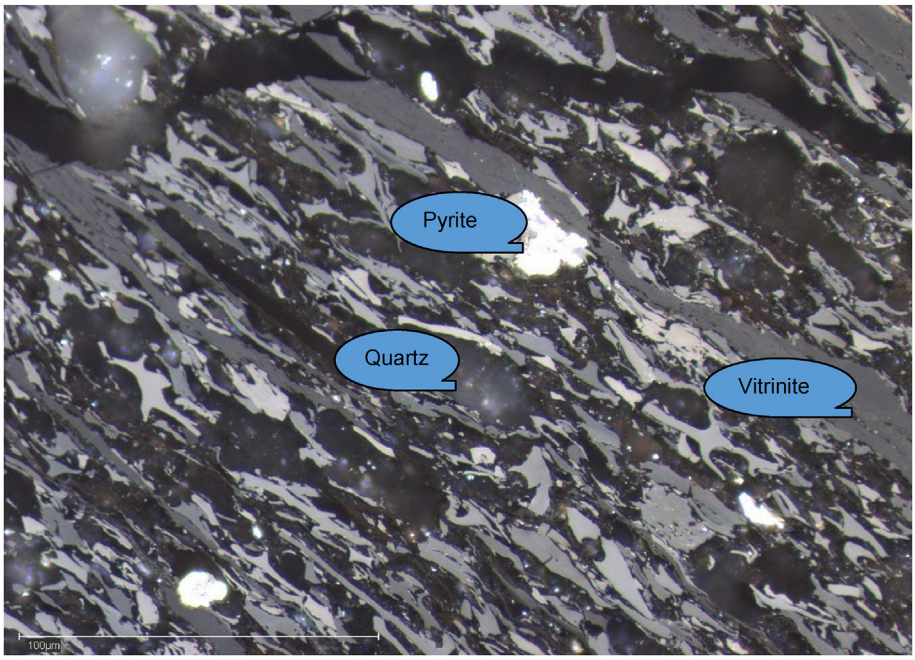

Fig. 4. Micrographs of pyrite, quartz and vitrinite observed in coal samples.

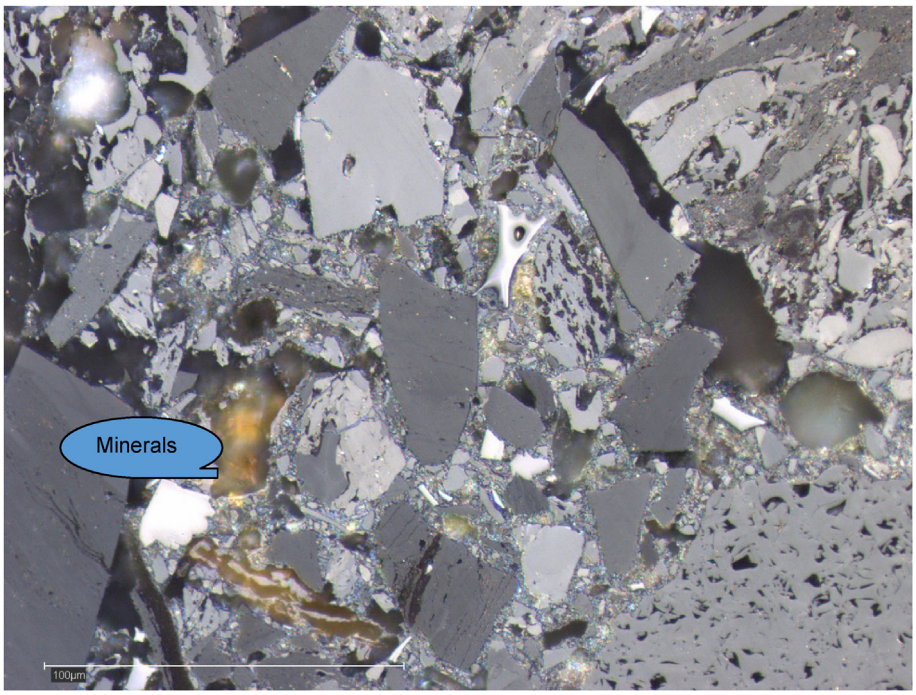

Fig. 5. Micrographs of minerals observed in the coal samples.

reflectance data indicates the coals samples are Medium Rank C (as per the UN-ECE in-seam classification scheme), also termed iso-rank, high volatile bituminous coal.

3.2. Proximate and ultimate analysis

The proximate analysis gives information concerning total moisture, ash, volatile matter and fixed carbon content by difference (weight %). The ultimate analysis gives elemental coal composition. Table 2 provide some insight into proximate and ultimate analysis data for the five coal samples. Sample 3 had a far higher ash content of about 34.45 wt% compared to the other four samples (average 32.41 wt%). However, the variations correlated reasonably well within the error of repeatability. Ash content influences ash deposition ash on the heat transfer surfaces of a coal-fired boiler. The buildup of ash deposits on the heat transfer surfaces of a coal-fired boiler is one of the key operational problems to be given attention for efficient and stable coal-fired operation. This interpretation is supported by the work of Park et al. [33], in which extreme ash content reduced boiler efficiency and, in severe cases can lead to shut-downs. Sample 5 had a higher carbon content of around 53.69 wt% compared to the other samples (average 51.81 wt %). Similar to ash content, the variation in values correlates reasonably well within the error of repeatability. Environmental pollutants such as sulphur dioxide, sulphuric acid and hydrogen sulphide have been connected to sulphur content in coal and as such, an understanding of the nature of the sulphur in the coal is very significant (Hancox and Götz [34]. All samples have a medium type of sulphur content in the range of 1.1–1.38 wt% as per coal classification closely related to sulphur content (1.0 to < 3.0 wt%). This result was similar to other coal analysis studies by Hancox and Götz [34], in which the average sulphur content of South African coals was found to be generally low.

Nitrogen is a major coal component inferior only to sulphur in

Table 2
Ultimate and proximate analysis (adb)

Analysis	Unit	Sample 1	Sample 2	Sample 3	Sample 4	Sample 5
Proximate Analysis						
Ash	(wt.%)	31.94	32.50	34.45	31.73	31.41
Volatile matter	(wt.%)	24.72	24.70	24.31	25.22	24.87
FC (by difference)	(wt.%)	38.13	36.67	35.22	36.97	37.57
Fuel Ratio		1.67	1.65	1.61	1.62	1.66
Ultimate Analysis						
Carbon	(wt.%)	51.55	50.88	50.24	52.66	53.69
Hydrogen	(wt.%)	3.33	3.37	3.36	3.33	3.35
Nitrogen	(wt.%)	1.01	1.00	0.97	1.00	1.04
Total sulphur	(wt.%)	1.21	1.20	1.10	1.38	1.35
Carbonates	(wt.%)	2.51	2.51	2.50	2.56	2.52
Oxygen (by difference)	(wt.%)	6.97	6.12	5.93	5.20	4.36
CV	(MJ/kg)	20.74	20.52	19.87	20.81	21.15
HI		52	51	50	50	54
AI		245	256	252	244	240
Total Moisture	(wt.%)	6.21	6.13	6.02	6.08	6.15

adb: air-dried basis; CV: Calorific value; HI: Hardgrove Index; AI: Abrasiveness Index; wt.% = weight%; FC: Fixed carbon.

the hazard it poses to the environment. All samples have a nitrogen content of about 1.00 wt%. A similar observation is also reported by Phiri et al. [35] who found that nitrogen content in coal occurs in minor proportion in the order of 2% or less. Hancox and Götz [34] showed that there is a direct correlation between vitrinite and nitrogen in individual coal bands, while an inverse correlation exists between inertinite and nitrogen. Both nitrogen and sulphur content are therefore positively correlated with the vitrinite maceral group in the Waterberg coal, increasing from west to east [34].

The coal samples had roughly the same moisture contents within the range of 6.02–6.21 wt.%. Higher moisture content in the coal is an undesirable constituent of coal because moisture reduces the heating value, and its weight adds to the transportation costs of coal.

It was noted that coal samples had calorific values in the range of 19.87–21.15 MJ/kg indicating heat liberated when these coals undergo complete combustion. The calorific value of coal samples studied can be estimated on the contribution of each element such as ash content, carbon content, hydrogen content and sulphur content. Hence, any change in ash content, carbon content, hydrogen content and carbon content decreases or increases the calorific value in the coal samples as per Dulong's formula in Eq. (1).

$$CV = 0.472C \times 1.30H \times 0.190S + 0.107A - 5.32 \quad (1)$$

where: C = carbon content, H = hydrogen content, S = sulphur content, and A = ash content.

Indirect measurement methods for calculating the calorific value include correlation-based methods and model-based methods. Using corresponding measured values for proximate analysis and ultimate analysis of five coal samples on Eq. (1), estimated calorific value values were quickly obtained as depicted in Fig. 6. The agreement between predictions from full-furnace coupled simulations and measured results is sufficient for engineering design purposes. The difference between the measured and estimated calorific values is the smallest in sample 1 and sample 2 with 0.26 and 0.44 respectively. A small standard error of the regression indicates that the data points are closer to the fitted values. However, the discrepancy between the measured and estimated calorific values is observed in samples 4 and sample 5. This discrepancy is usually caused by overfitting. Overfitting denotes a model that fits the training data very good to lose some generalization capability [36]. The contribution to a large difference between the measured calorific value and estimated calorific value can be attributed to the carbon content and hydrogen variation in samples. Carbon and hydrogen content are the main combustible elements in coal. Carbon content is the predominant one on a weight basis as it constitutes 60–95% of the coal. Due to the high carbon content in sample 4 and sample 5, a calorific value significantly increased. From the data the higher the ash content value, the lower the calorific value. Otherwise, the lower the ash content value, the higher the calorific value. Furthermore, high sulphur content also affects the heating value which adds to the increased calorific value in sample 4 and sample 5.

Coal properties affect the boiler's availability, reliability, and efficiency, consequently, impacting the economics along with the short and long-term operation of the plant. All samples have volatile matter content of around 24.74 wt%. During combustion, the quantity and composition of the volatile matter determine the luminosity and stability of the flame [31]. It has been reported that an industrial burner design dearly depends on the amount and quality of the volatile matter [31]. Subsequently, coals with high volatile matter require serious attention under high ambient atmospheric temperatures as it is susceptible to spontaneous combustion. This interpretation is supported by the work of Santhosh Raaj et al. [37], in which mill inlet temperature must be carefully maintained to ensure drying of coal as well as to avoid mill fire when handling coal with the high volatile matter. However, when firing medium volatile coals, the tempering air quantity could be reduced to gain the heat pickup in the air heater, which leads to an increase in the boiler efficiency [37]. The ratio of fixed carbon to volatile matter, best known as the fuel ratio, shows the combustion characteristics of the coal. The lower the fuel ratio, (i.e. average 1.63 as in the current study), the better the the ease of ignition and burnout.

Coal grindability traditionally measured by Hardgrove Grindability Index (HGI) is of intense interest given that it serves as a predictive tool to regulate the performance capacity of industrial pulverisers in the power station. Usually, coal grindability characteristics reveal the coal hardness, tenacity, and fracture which are influenced by coal rank, petrography, and the distribution and the types of minerals [38]. The average HGI for all samples is about 51. According to Snyman [31], the HGI of coal depends on its elemental composition, macromolecular structure and on the degree of cohesion between the different maceral and mineral grains of which it is comprised. The relatively high correlation coefficient attained when the HGI is articulated relating to the total carbon and

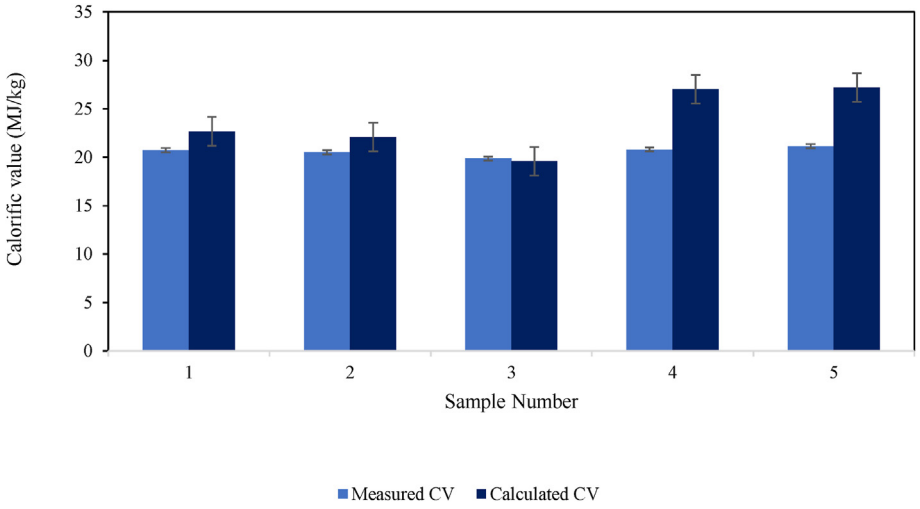

Fig. 6. Comparing estimated and measured calorific values of the investigated coal samples.

hydrogen contents indicates that the mineral matter content plays a very subordinate role from this point of view. On the other hand, the coal abrasiveness is a measure of how abrasive the coal is to the mill internals to minimize the wear rate. For the coal samples studied, the abrasiveness index ranged between 240 and 256. Now that an understanding of the proximate and ultimate data has been obtained, it is essential to acquire an understanding of the coal qualities impact occurring during combustion in a boiler. Both the proximate and ultimate analysis numbers amounted to 100% as shown in Table 2.

3.3. Coal ash oxide analysis

Table 3 shows the elements of coal ash oxide from power plant coal samples determined using Philips PW2404 X-ray fluorescence (XRF) spectrometer. Ash oxide chemical components are mainly made up of heavy metal elements such Al_2O_3, CaO, Fe_2O_3, and SiO_2; along with trace elements such TiO_2, MnO and P_2O_5. It is clear from Table 3 that the dominant oxides are silica (SiO_2) and alumina (Al_2O_3) like what was published by Yusuff et al., [39]. MnO and K_2O appear in minor proportion. This is consistent with a similar observation by Wagner and Tlotleng [40] who found that the ash chemistry is controlled by SiO_2 and Al_2O_3 (52–62.4 wt.% and 22.5–36.7 wt.% respectively).

3.4. The effect of O_2 on SO_2 concentration

The O_2 concentration plays a major role in determining the behavior of the combustion process. As already stated in the introduction, coal contains sulphur and upon combustion, different sulphur forms present in coal release sulphurous gases as per reactions 2–5.

$$SO_4^{2-} + ½O_2 \rightarrow \text{Oxides} + SO_2 \quad (2)$$

$$SO_3^{2-}\text{Sulphide} + O_2 \rightarrow \text{Oxides} + SO_2 \quad (3)$$

$$FeS + 2H^+ + O_2 \rightarrow Fe^{2+} + H_2S + SO_2 \quad (4)$$

$$S + O_2 \rightarrow SO_2 \quad (5)$$

The O_2 concentration was varied between 2.70 vol% and 3.78 vol % to establish its impact on SO_2 emissions. Fig. 7 shows the effect of O_2 concentration on SO_2 emissions measurements under different boiler loads. It is revealed that under 100% BMCR condition, increasing O_2 concentration from 2.7 vol% to 3.28 vol% during combustion decreases SO_2 concentration from 3862 mg/Nm^3 to 2841 mg/Nm^3. However, increasing O_2 concentration beyond 3.28 vol%, SO_2 concentration increased from 2841 mg/Nm^3 up to 3601 mg/Nm^3 at 3.65 vol% and 3.78 vol% which is outside the target of <3500 mg/Nm^3. The former part of the insignificant reduction of SO_2 concentration at 2.70 vol% up until 2.87 vol% can be attributed to no excess air (stoichiometry), then SO_2 concentration improved in reduction with the increase in O_2 concentration beyond 2.87 vol% reflecting above stoichiometric condition. Such a finding would suggest that the sulphur content is transformed to SO_2 and SO_3 in a specific condition, during the combustion process [41]. Similar results were also reported in the earlier investigation by Rahat et al. [6] who suggested that various combustion parameters, such as O_2 percentage, airflow rate and distribution and load, etc., may be adjusted to realize lower rates of emissions produced during the combustion process. During the latter three samples, SO_2 concentration reduction remained invariable at 3472–3601 mg/Nm^3. The increase in SO_2 concentration beyond the O_2 concentration of 3.28 vol% is potentially due to higher O_2 contents in the reactor making the combustion of volatile gases more enhanced, leading to an increase in SOx emissions. Moreover, the sulphur content that is not released as SO_2, H_2S, COS or CS_2 is either retained in the char or contained in the ash [35]. Therefore, a significant improvement in the reduction of SO_2 concentration is achieved when the O_2 concentration is 3.28 vol%.

In the case of 60% BMCR condition (Fig. 8), a similar pattern was observed whereas O_2 concentration increases, SO_2 concentration reduced up to O_2 concentration of 3.08 vol%. However, because of the reduced load, O_2 concentration requirements were also reduced. Furthermore, it is important to note that the boiler load (60% BMCR and 100% BMCR) and state of the boiler cleanliness (dirty or clean inner surfaces) affect the SO_2 emissions concentrations. These findings are quite desirable as environmental regulations are stricter regarding power generation operations.

3.5. Effect of coal flow on SO_2 concentration

The amount of SO_2 concentration produced can be calculated from the total amount of coal burnt during the combustion as per Eq. (6):

$$SO_2 = \left(\frac{m_{coal} \times \left(\frac{S}{100} \times \frac{1000}{32.064}\right)}{100 \times 64.0628} \right)_{\text{kg/kg Coaldry}} \quad (6)$$

where: m = coal mass flow (Tons/hr), S = sulphur content (wt.%)

The effect of various coal flows such as 281–320 tonnes/hr range on SO_2 concentration was undertaken and the obtained results are illustrated as depicted in Fig. 9. It can be seen from Fig. 9 that as expected, SO_2 concentration remained constant at 3862 mg/Nm^3 when coal mass flow remained constant at 320 Tonnes/hr. Moreover, decreasing the coal flow from 320 to 299 Tonnes/hr gradually reduced SO_2 concentration from 3862 mg/Nm^3 to 3284 mg/Nm^3 meaning that when the coal mass decreases, less SO_2 concentration is released during the combustion process. Interestingly, with a further reduction of coal flow from 299 Tonnes/hr to 281 Tonnes/hr, further reduction of SO_2 concentration from 3284 mg/Nm^3 to 2965 mg/Nm^3 was noted which is desirable. Samples 1, 2 and 10 present a condition where SO_2 concentration exceeded the target limits and coal mass was adjusted to reduce the SO_2 concentration. By reducing the coal mass flow from 320 to 281 Tonnes/hr, high SO_2

Table 3
Ash Oxides (wt.%, adb).

Analysis	SiO_2	Al_2O_3	Fe_2O_3	TiO_2	P_2O_5	CaO	MgO	Na_2O	K_2O	SO_3	MnO
Target	58.24	27.8	5.89	1.21	0.35	3.13	1.11	0.11	0.13	2.16	0.005
Sample 1	56.0	26.0	6.40	1.44	0.38	4.20	1.15	0.08	1.80	2.20	0.04
Sample 2	57.9	26.5	5.41	0.46	4.4	1.2	0.1	0.8	1.2	2.8	0.03
Sample 3	57.1	27.1	5.4	1.4	0.52	4.1	1.1	0.1	0.8	2.3	0.03
Sample 4	55.2	25.7	7.0	1.40	0.48	4.5	1.2	0.1	0.8	2.4	0.04
Sample 5	55.4	26.4	6.5	1.4	0.53	4.7	1.3	0.1	0.8	2.3	0.03

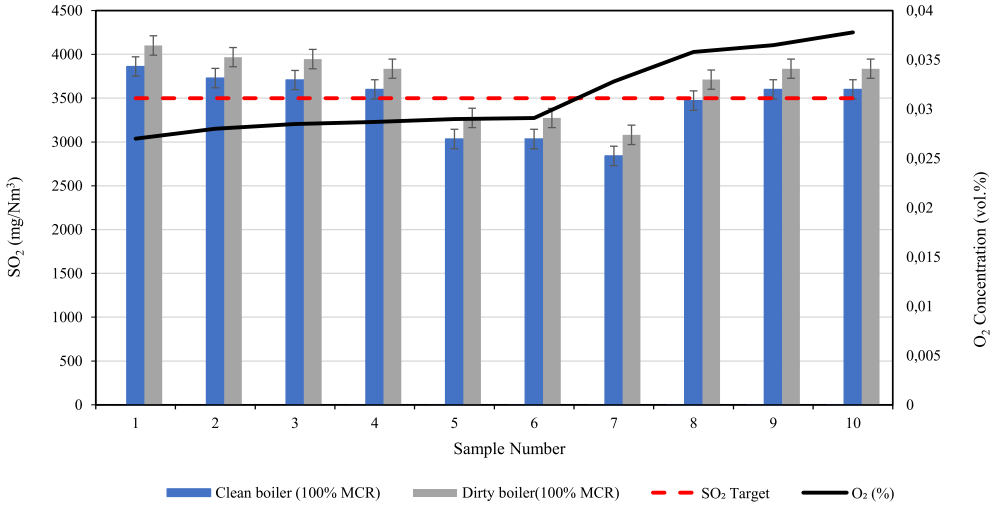

Fig. 7. The SO_2 concentration measurements at 100% BMCR and various O_2 concentration.

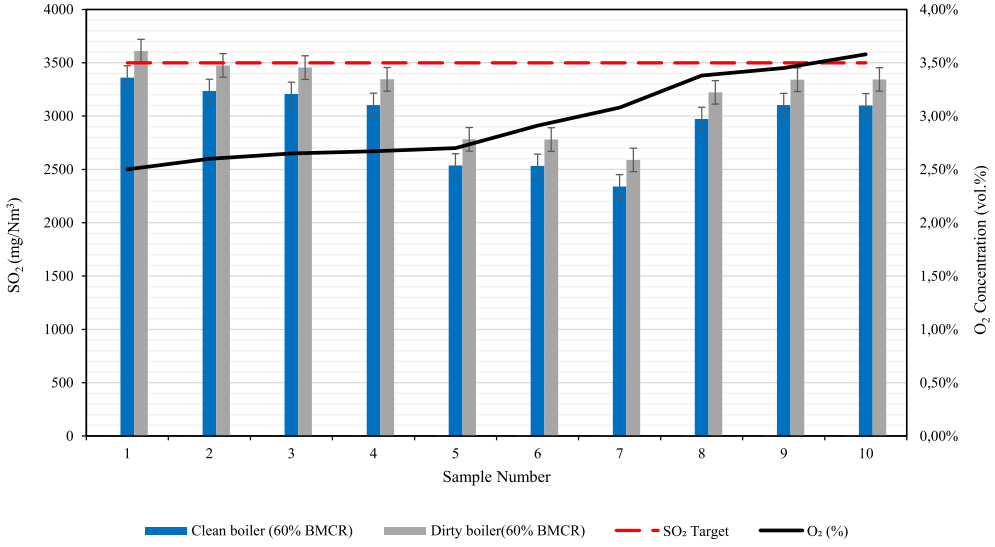

Fig. 8. The SO_2 concentration measurements at 60% BMCR and various O_2 concentration.

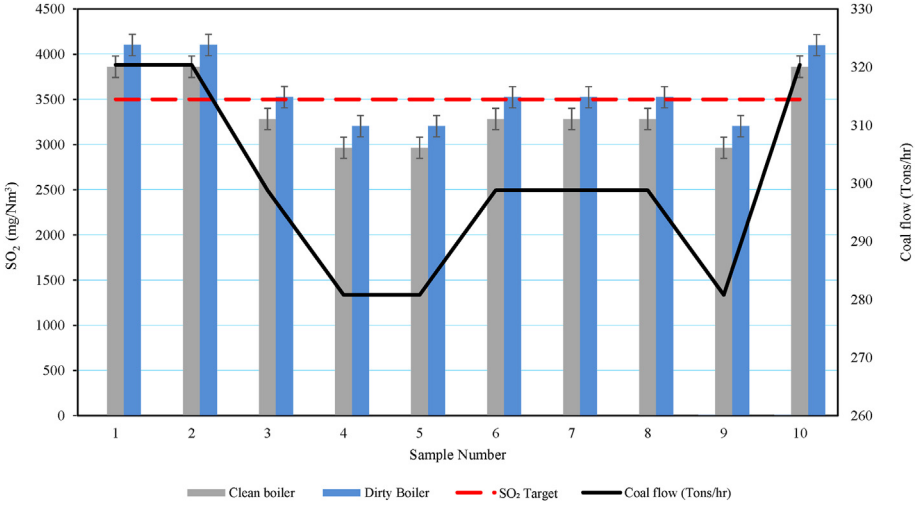

Fig. 9. A comparison of the sulphur dioxide concentration measurements at various mass flow, SO_2 concentration normalized to 6% O_2.

concentration was reduced from 3862 mg/Nm^3 to 2965 mg/Nm^3 which is within the target of 3500 mg/Nm^3. This suggests that SO_2 concentration is the most sensitive to coal mass flow, hence reducing coal mass flow has greater potential for reduction of SO_2 emissions. However, reducing coal mass flow impacts load generation. Therefore, as coal mass reduces, boiler load reduces correspondingly. Nevertheless, at a reduced coal mass, Verma et al. [42] emphasized that uncontrolled CO and dust emissions are expected by most boilers which is less desirable. This is because increasing the coal flow does not produce a monotonic decreasing trend in the ignition distance of the fuel/air flow but that there is an optimal concentration that provides the shortest distance [43].

3.6. Effect of air/fuel ratio on NOx

Coal generally contain nitrogen, and this becomes a source of NOx during combustion [43]. The air/fuel ratio is an important operating parameter, which not only affects NOx formation but also boiler thermal efficiency. The production of nitric oxide (NO) during the combustion process is three-fold, i.e., thermal nitric oxide, prompt nitric oxide and fuel nitric oxide [44]. According to Li et al. [44], NO_x involves a lot of species with the most important being NO, NO_2, N_2O, NH_3 and HCN. NO normally amounts to at least 90% of the NOx produced. However, the emission of NOx coming from the combustion process is a result of complex factors and the result of competing formation/destruction processes [43]. The mechanisms of NO formation have been a topic of many investigations and the literature in this area is well established. General NO formation mechanisms are summarized as per reactions 7–9:

$$O + N_2 \leftrightarrow NO + N \tag{7}$$

$$N + O_2 \leftrightarrow NO + O \tag{8}$$

$$N + OH \leftrightarrow NO + H \tag{9}$$

NOx production at different air/fuel ratio during the combustion process can be evaluated as shown in Eq.s 10–12:

$$Air \Big/ Fuel\ Ratio = \frac{\sum(Air\ Flow)}{Fuel\ Flow} \tag{10}$$

$$Air \Big/ Fuel\ Ratio = \frac{\sum(Primary\ Airflow; Total\ Secondary\ Airflow)}{Coal\ Flow} \tag{11}$$

For example, the emissions of NOx (at 6% O_2) can be calculated from measured NO and O_2 concentrations according to Eq. (12).

$$NO_x = \frac{NO(ppm)}{0.95} \times \frac{46\ \left(\frac{g}{mol}\right)}{22.4\ \left(\frac{L}{mol}\right)} \times \frac{21-6}{21-O_2} \tag{12}$$

Fig. 10 depicts the NOx production at different air/fuel ratio, with the coal combustion. Considering the 100% BMCR clean boiler scenario, the concentration of NOx decreased with air-to-fuel ratio advancement. It should be noted that NOx formation decreases by a large margin when the air/fuel ratio changes from the lean side (i.e., 7.14–7.23) to the rich side (i.e., 7.24–7.29). For instance, at the air/fuel ratio of 7.14, the NOx emissions decreased from 350 mg/Nm^3 to 332 mg/Nm^3 at the air/fuel ratio of 7.24. However, further reduction with some quasi-steady-state has been observed when the air/fuel ratio goes beyond 7.24. The peak value of NOx reduction usually occurs at the rich side, namely among the range of 7.24–7.29. It can therefore be concluded that the effect of NOx emissions become more significant with decreasing NOx emissions with increasing air/fuel ratio factor. Such conduct could be attributed to the nitrogen content transformed to NO_2 and in a specific condition to NO during the coal combustion process [41]. A similar observation is also reported by Krzywanski et al. [43], when studying the nitrogen to NOx conversion which grew with the rise in oxygen content in the flue gas, leading to higher NOx emissions. This observation is also in line with the findings by Kuang et al. [44] who evaluated the effects of staged air and overfire air on NOx emissions and carbon burnout in a down-fired 600 MW boiler. Kuang et al. [44] determined that increasing the amount of air sent to the combustion chamber leads to an increase in the amount of NOx emissions. However, for the 100% BMCR dirty boiler scenario, there was a similar pattern as the clean boiler only that the NOx emissions were 10 mg/Nm^3 higher on average. High NOx emissions in the dirty boiler can be attributed to soot deposits on inner surfaces which affect the exhaust gas temperature the steam quality and emissions. Furthermore, this finding is in agreement with de Diego et al. [45] who studied NOx emissions from regenerator of calcium looping process. The increase rate of NOx emissions for 60% BMCR situation is seen to be haphazard. However, the lowest NOx emissions were obtained for the air/fuel ratio of 7.20 while the highest were obtained for the air/fuel ratio of 7.14; 7.26; 7.26 and 7.29. The main reason for NOx haphazard increase is because under low-load conditions, the gas temperature decreases, the ignition position is farther away, and the degree of burnout varies significantly [46]. Jiang et al. [47], further added that although the excess air coefficient needs to be maintained within a relatively high range to ensure the stability of the flame, high excess air causes the oxide concentration to increase. Like the 100% BMCR dirty boiler scenario, 60% BMCR dirty followed a similar pattern as the clean boiler only that the NOx emissions were 4 mg/Nm^3 higher on average.

3.7. The effect of coal calorific value and O_2 concentration on boiler thermal efficiency

Fig. 11 depicts 100% BMCR efficiency as a function of O_2 concentration. As O_2 concentration increased from 2.70 vol% to 3.78 vol %, boiler efficiency increased although its increase is not necessarily following a certain pattern. The highest boiler efficiency of 90.82% was attained at an O_2 concentration of 3.28 vol% for a 100% BMCR clean boiler. Similarly, for the 100% BMCR dirty boiler situation, the highest boiler efficiency of 90.25% was attained. Fig. 12 shows 60% BMCR efficiencies as a function of O_2 concentration. As O_2 concentration increased from 2.50 vol% to 3.58 vol%, boiler efficiency increased although its increase is not necessarily following a certain pattern. The highest boiler efficiency of 90.82% and 89.84% for 60% BMCR clean boiler and 60% BMCR dirty boiler respectively was attained at an O_2 concentration of 3.08 vol%. According to Li et al. [14], reduction of oxygen concentration results in incomplete combustion of the fuel and high unburned carbon in the fly-ash, thereby reducing boiler efficiency.

Fig. 13 depicts boiler efficiencies as a function of coal calorific value. By increasing the calorific value from 19.3 MJ/kg to 20.80 MJ/kg, boiler efficiency did not necessarily follow a specific pattern for the increase but improved from 90.0% to 90.82%. The highest calorific value of 20.5 MJ/kg resulted in the highest efficiencies on a 100% BMCR boiler. As for 60% BMCR boiler, the highest efficiencies were attained at the different calorific values of 20.7 MJ/kg and

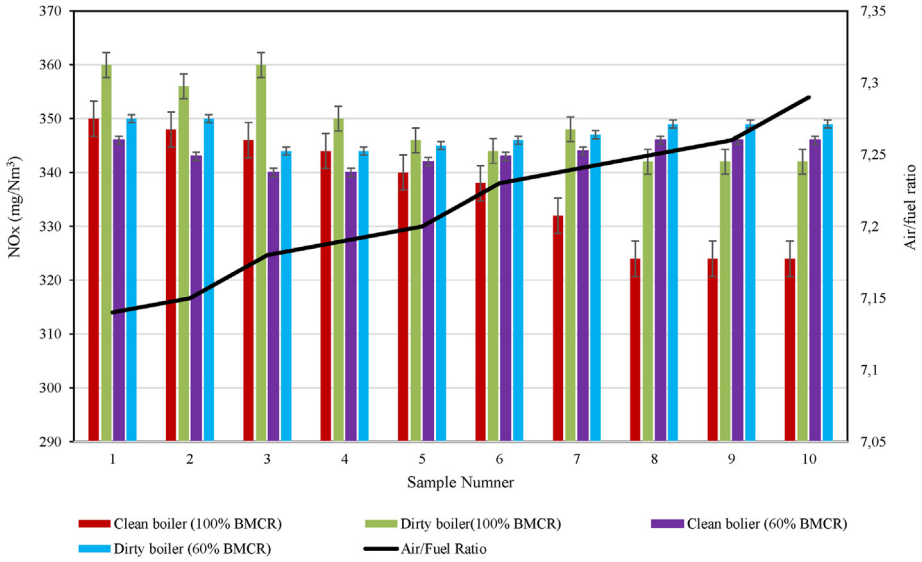

Fig. 10. NOx production at the different air-fuel ratios, NOx emissions normalized to 6% O_2.

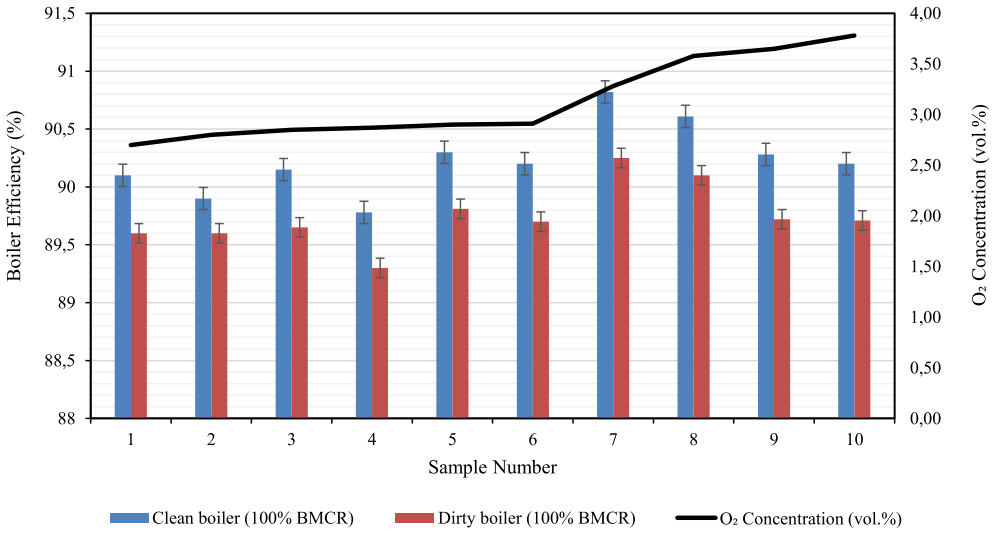

Fig. 11. The 100% BMCR efficiency as a function of O_2 concentration.

20.8 MJ/kg for efficiencies of 90.46% and 89.84% at the clean boiler and dirty boiler respectively. The higher the calorific value, the lesser would be the consumption of coal for an equal amount of power, reducing the emission from the power plant and contributing to a better environment. The results of the current study are consistent with the view of Verma et al. [42] who highlighted that uncontrolled CO and dust emissions are expected due to high O_2 concentration resulting in lower combustion efficiency which is less desirable.

3.8. Boiler thermal efficiency calculations and heat losses

It is crucial to know the boiler performance which specifies the effectiveness of the heat exchanger of the boiler that transfers the heat energy from the fireside to the waterside. The overall boiler efficiency depends on many more parameters apart from combustion and thermal efficiencies. Therefore, testing of the boiler efficiency calculates the best possible appropriate efficiency so that corrective action could be taken, to rectify the observed problem areas. In actual practice, two methods are commonly used to find out boiler efficiency, namely the direct method, and the indirect method of efficiency calculation. The indirect efficiency of a boiler is calculated by finding out the individual losses taking place in a boiler and then subtracting the sum from 100%. This method involves finding out the magnitudes of all the measurable losses taking place in a boiler by separate measurements. The losses calculated include stack losses, radiation losses, blowdown losses etc. What is meant by the indirect calculation of boiler efficiency is a calculation that does not directly involve the formulation of the main components of the input and output boiler efficiency energy, but by calculating the losses that exist. Considering the following Eq [13]. for direct method:

$$\eta_{Boiler} = \frac{(Heat\ in\ Steam)}{(Heat\ in\ Fuel)} \quad [13]$$

where:

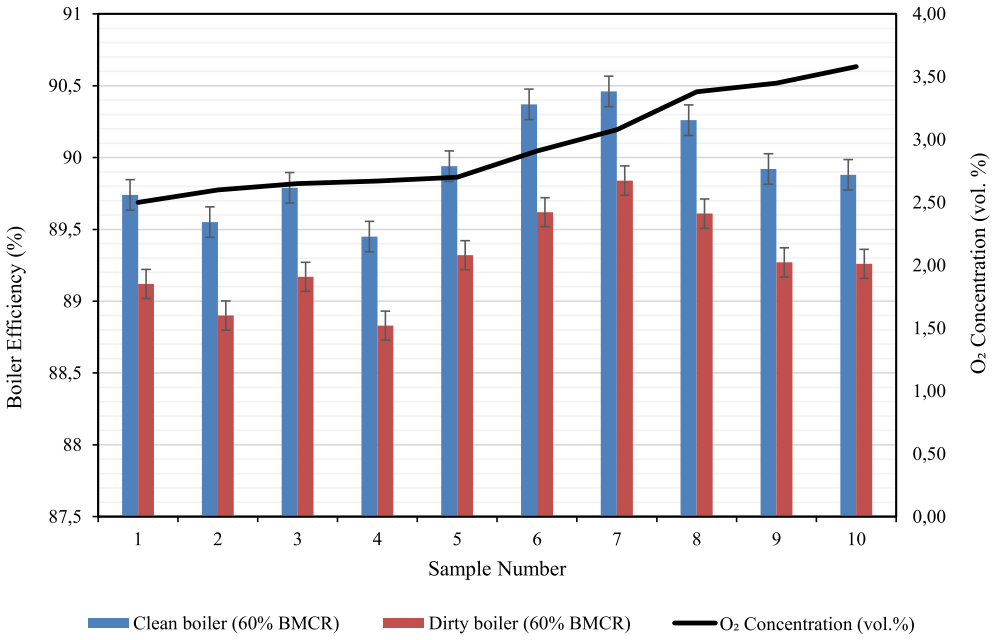

Fig. 12. The 60% BMCR efficiency as a function of O_2 concentration.

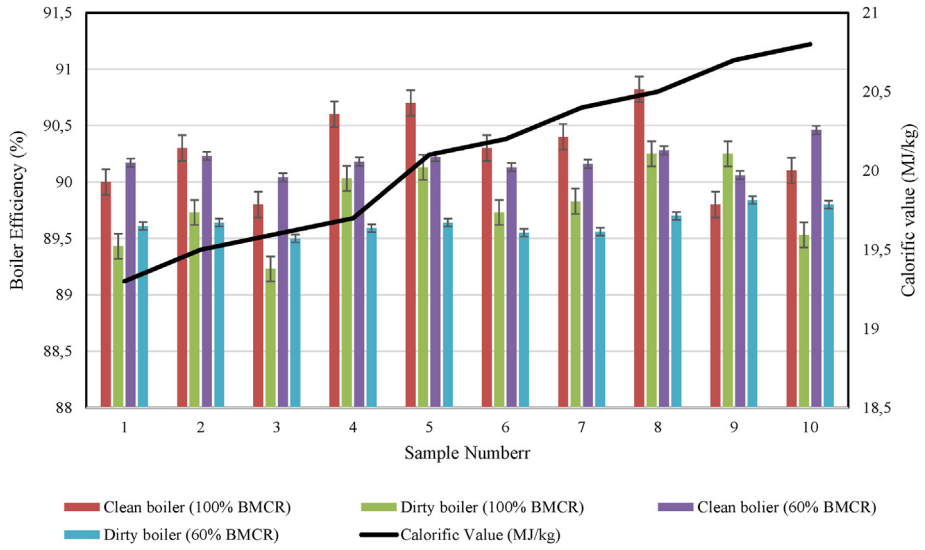

Fig. 13. Boiler efficiency as a function of coal calorific value.

$$Heat\ in\ Steam = (\Delta H_{MS-}\Delta H_{FW}) \times m_{MS} + (\Delta H_{RO} m_{RO}) - [\times (\Delta H_{RI} m_{RI}) + (\Delta H_{RSW} m_{RSW})] \quad [14]$$

$$Heat\ in\ Fuel = [(M_{CB} \times CV_C) + (M_{OB} \times CV_O)] \quad [15]$$

Substituting Eqs [14,15]. on Eq [13]. gives:

where:ΔH_{MS} = Main steam enthalpy (kJ/kg), ΔH_{FW} = Feed water enthalpy (kJ/kg), m_{MS} = Main stream flow (kg/s), ΔH_{RO} = Re-heater outlet enthalpy (kJ/kg), m_{RO} = Re-heater outlet flow (kg/s), ΔH_{RI} = Re-heater inlet enthalpy (kJ/kg), m_{RI} = Re-heater inlet flow (kg/s), ΔH_{RSW} = Re-heater spray water enthalpy (kJ/kg), m_{RSW} = Re-heater spray flow (kg/s), M_{CB} = Coal burnt for boiler (Tons), M_{OB} = Oil burnt for boiler (Tons), CV_C = Calorific value of coal (MJ/kg), CV_O = Calorific value of oil (MJ/kg)

$$Boiler = \frac{(\Delta H_{MS-}\Delta H_{FW}) \times m_{MS} + (\Delta H_{RO} m_{RO}) - [(\Delta H_{RI} m_{RI}) + (\Delta H_{RSW} m_{RSW})]}{[(M_{CB} \times CV_C) + (M_{OB} \times CV_O)]} \quad [16]$$

Table 4
Coal, water, and steam variables of each case.

Parameter	Unit	60% BMCR Clean Boiler	60% BMCR Dirty Boiler	100% BMCR Clean Boiler	100% BMCR Dirty Boiler
Percentage MCR	(%)	60	60	100	100
Generator Load	(MW)	543	540	670	666
Total boiler steaming time	(Hr)	24	24	24	24
Coal mass	(Tons)	7090	7090	8050	8050
CV Coal	(MJ/kg)	20.74	20.52	20.81	20.74
O_2 Concentration	(%)	3.08	3.08	3.28	3.28
Fuel/air ratio		7.25	7.25	7.25	7.25
Total steam flow at the re-heater outlet	(kg/s)	30352320	29479680	50502960	51088320
Total steam flow at the re-heater inlet	(kg/s)	22894400	22859200	43602000	43545600
Total spray water flow	(kg/s)	440640	613440	974128	986688

BMCR = boiler maximum continuous rating.

Table 5
Operating values in boiler efficiency performance testing of a once-through boiler.

Parameter	Unit	Case 1 60% BMCR Clean Boiler	Case 2 60% BMCR Dirty Boiler	Case 3 100% BMCR Clean Boiler	Case 4 100% BMCR Dirty Boiler
Main steam flow	(kg/s)	39707×10^6	39868×10^6	45962×10^6	44001×10^6
Main steam temperature	(°C)	535.4	535.3	536.5	536.4
Main steam pressure	(Bar)	144	144	172	172
Main steam enthalpy	(kJ/kg)	3417.3	3417.1	3388.6	3388.3
Feedwater temperature	(°C)	235.5	234.2	248.9	247.1
Feedwater enthalpy	(kJ/kg)	1015.7	1010.5	1080.3	1071.6
Re-heater outlet flow	(kg/s)	351.3	341.2	531.4	519.3
Re-heater outlet temperature	(°C)	537.0	537.1	537.7	537.6
Re-heater outlet pressure	(Bar)	31.29	30.80	40.0	39.30
Re-heater outlet enthalpy	(kJ/kg)	3539	3539.7	3532.1	3532.8
Re-heater inlet flow	(kg/s)	346	328	521	504
Re-heater inlet temperature	(°C)	328	328	328	328
Re-heater inlet pressure	(Bar)	31.4	30.3	35.1	34.2
Re-heater inlet enthalpy	(kJ/kg)	3060.1	3062.9	3050.4	3039.5
Re-heater spray temperature	(°C)	168	168	168	168
Re-heater spray enthalpy	(kJ/kg)	710.5	710.5	710.5	710.5
Boiler efficiency	(%)	90.46	89.84	90.82	90.25
Sulphur dioxide	(mg/Nm^3)	2340	2589	2841	3081
Oxides of nitrogen	(mg/Nm^3)	346	349	324	342

Using Eq [16] and coal, water, and steam operating values for various scenarios in Table 4 as well as operating values in boiler efficiency performance testing of once-through boiler in Table 5. As shown in Table 5, four cases are considered in the current study. Case #1 is the clean boiler at 60% boiler maximum continuous rating (BMCR), case #2 is the dirty boiler at 60% BMCR. Case #3 is the clean boiler at 100% BMCR and case #4 is the dirty boiler at 100% BMCR. The lowest load for which design data was available is 60% BMCR, hence this selection. The lowest boiler efficiency of 89.84% was noted at case #2 at operating conditions for a lower load of 60% BMCR for a dirty boiler and the highest boiler efficiency of 90.82% was noted at case #3 at operating conditions for a full load of 100% BMCR for a clean boiler. This increase in boiler efficiency at full load is attributed to the improvement of combustion conditions in the boiler, the enhancement of pulverized-coal burnout, and the reduction of carbon in fly ash and slag, which reduce the heat loss from solid incomplete combustion significantly. The results are in good agreement with the findings of Mendes et al. [48] who established that ash deposits on the convection surfaces of the tubes reduce the heat transfer from the hot gases to the steam and, consequently, decrease the efficiency of the steam generator [48]. Therefore, excessive ash deposits reduce boiler efficiency and, in extreme cases, may lead to power plant shut-down. To achieve high boiler efficiency, it is desirable to reduce the flue gas heat loss by lowering the flue gas temperature.

During boiler operation of a coal-fired power plant, the heating surface will inevitably generate fouling or slagging, thus affecting the overall heat transfer on surfaces. Fig. 14 shows the effect of soot blowing on flue gas exit temperature from 100 °C to 1200 °C as a function of plant operation. The flue gas exit temperature varied as a function of reduced load and maximum operational load. All these cases use the same concentration of O_2 and air/fuel ratio as well as varied coal mass flow. When the load decreased from 100% to 60%, the instantaneous coal mass flow rate decreased. The results show that compared to the dirty boiler, fuel consumption in a steady-state regime at the same loads, the actual specific fuel consumption decreased during load reduction to 60% BMCR. On the other hand, during load increases, the specific fuel consumption increased even more. The major boiler heat loss is the heat of the exit flue gas and has been felt at the lower levels of the power plant including from furnace exit temperature to economizer exit. However, in the case of the stack, ESP inlet and secondary air heater gas outlet flue gas exit temperature, the effect of clean versus dirty were negligible. Therefore, the state of the boiler cleanliness or dirt affect the exhaust gas temperature, improve the boiler efficiency, ensure steam quality, reduce SOx and NOx emissions, and prolong the life of the boiler heating pipe.

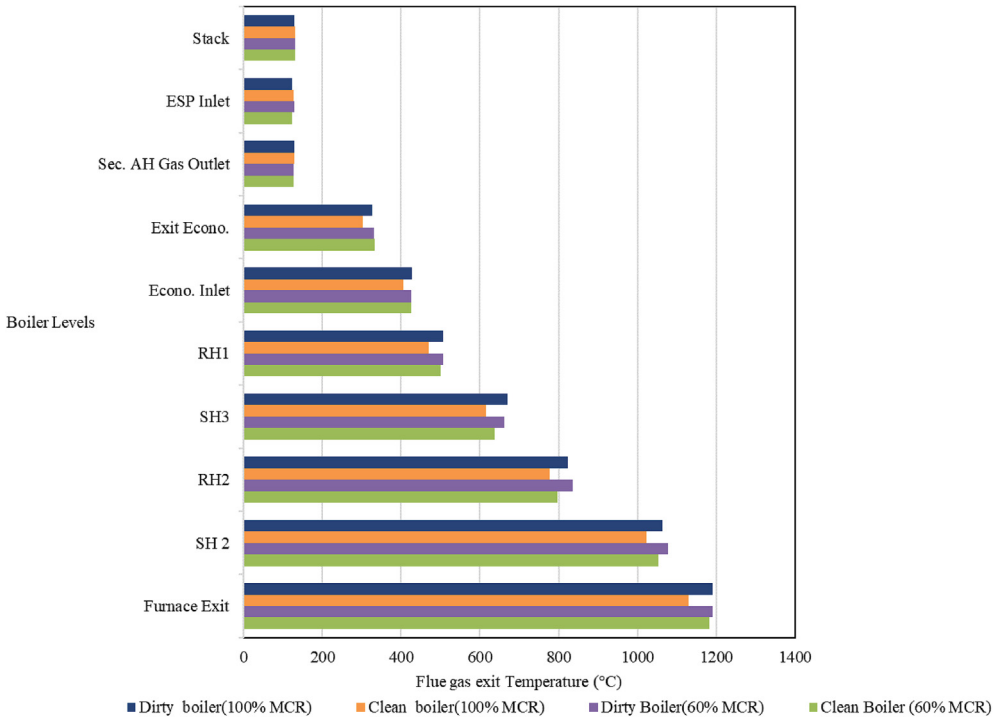

Fig. 14. The effect of dirty and clean boiler on flue gas exit temperature.

4. Conclusions

Simultaneous reduction of NOx emission and SOx emission aided by improved efficiency of a Once-Through Benson Type Coal Boiler was observed. The effects of input parameters (coal calorific value, inlet O_2 concentration in boiler, coal mass flow rate and air/fuel ratio) on output parameters (heat loss, SOx and NOx emissions, thermal efficiency of dirty and clean boiler at different loads) were established. A significant improvement in the reduction of SO_2 concentration is achieved when the O_2 concentration is 3.28 vol% and the coal mass flow rate is equal to 281 tonnes/hr. NOx concentrations are reduced by a large margin when the air/fuel ratio changes from the lean side (i.e., 7.14) to the rich side (i.e., 7.29). The optimum air/fuel ratio of 7.24 resulted in NOx reduction. Therefore, the state of the boiler cleanliness (dirty or clean inner surfaces) affects the exhaust gas temperature, improve the boiler efficiency, ensure the steam quality, reduce SOx and NOx emissions and prolong the life of the boiler heating pipe. Obtained results could help to optimize the operation of the whole power plant and make it possible to make better decisions when planning the plant operation that will have a positive environmental and financial impact due to possible savings in running an ageing generation fleet. The results of this study emphasize the possibility to increase the efficiency of an older coal-fired boiler (like a once-through Benson type coal boiler) cost-effectively, especially when space or capital budgets are limited.

Credit author statement

Malebo Mollo: Investigation; Methodology; Writing – original draft; **Seshibe Makgato:** Conceptualization, Resources, Writing - review & editing and Co-supervision; **Andrei Kolesnikov:** Formal analysis and Supervision.

Declaration of competing interest

The authors declare that they have no known competing financial interests or personal relationships that could have appeared to influence the work reported in this paper.

Nomenclature

m	coal mass flow (Tons/hr)
S	sulphur content (wt.%)
η	Boiler Fuel Efficiency (%)
Q_{steam}	Total heat energy absorbed by water vapor (calories, Joule)
Q	Discharge of water vapor out of boiler (kg/h)
h_f	Steam enthalpy out of boiler (kJ/kg)
h_g	Water enthalpy entering boiler (kJ/kg)
Q_{fuel}	The heat energy produced by fuel burning (kJ)
C	carbon content (wt.%)
CV	Calorific Value (MJ/kg)
adb	air-dried basis
ΔH	specific enthalpy of working medium (kJ/kg)
p	steam pressure (MPa)
ΔH_{MS}	Main Steam Enthalpy (kJ/kg)
ΔH_{FW}	Feed Water Enthalpy (kJ/kg)
m_{MS}	Main Steam Flow (kg/s)
ΔH_{RO}	Re-heater outlet Enthalpy (kJ/kg)
m_{RO}	Re-heater outlet Flow (kg/s)
ΔH_{RI}	Re-heater inlet Enthalpy (kJ/kg)
m_{RI}	Re-heater inlet Flow (kg/s)
ΔH_{RSW}	Re-heater spray water Enthalpy (kJ/kg)
M_{RSW}	Re-heater spray Flow (kg/s)
M_{CB}	Coal burnt for boiler (Tons)
M_{OB}	Oil burnt for boiler (Tons)
CV_C	Calorific Value of Coal (MJ/kg)
CV_O	Calorific Value of Oil (MJ/kg)

A	ash content (wt.%)
H	hydrogen content (wt.%)
wt.%	weight percent
BMCR	boiler maximum continuous rating

Appendix A. Supplementary data

Supplementary data to this article can be found online at https://doi.org/10.1016/j.energy.2022.123551.

References

[1] Wang C, Liu Y, Zheng S, Jiang A. Optimizing combustion of coal fired boilers for reducing NOx emission using Gaussian Process. Energy 2018;153:149–58.
[2] Li Z, Miao Z, Shen X, Li J. Effects of momentum ratio and velocity difference on combustion performance in lignite-fired pulverized boiler. Energy 2018;165:825–39.
[3] Bekker B, Eberhard A, Gaunt T, Marquard A. South Africa's rapid electrification programme: policy, institutional, planning, financing and technical innovations. Energy Pol 2008;36:3125–37.
[4] StatsSa. Census. Census in brief. Pretoria: Statistics South Africa; 2011. 2012.
[5] Gu H, Zhu H, Cui Y, Si F, Xue R, Xi H, Zhang J. Optimized scheme in coal-fired boiler combustion based on information entropy and modified K-prototypes algorithm. Results Phys 2018;9:1262–74.
[6] Rahat AAM, Wang C, Everson RM, Fieldsend JE. Data-driven multi-objective optimisation of coal-fired boiler combustion Systems. Appl Energy 2018;229:446–58.
[7] Gani A, Wattimena Y, Erdiwansyah Mahidin, Muhibbuddin Riza M. Simultaneous sulfur dioxide and mercury removal during low-rank coal combustion by natural zeolite. Heliyon 2021;7:070522.
[8] Gupta PK. Environmental and ecotoxicology, illustrated toxicology with study questions. E-Publishing Inc., Academic Press; 2018. p. 373–425.
[9] Xie P, Li CL, Shao B, Xu XJ, Chen XD, Zhao L, Zhou X, Lee DJ, Ren NQ, Chen C. Simultaneous removal of carbon dioxide, sulfur dioxide and nitric oxide in a biofilter system: optimization operating conditions, removal efficiency and bacterial community. Chemosphere 2021;276:1300842.
[10] Prayuenyong P. Coal biodesulfurization processes. Songklanakarin J Sci-Technol 2002;24:493–507.
[11] Government Notice No.248, 31 March 2010 National environmental management: air quality act. 2004. p. 11 (ACT NO. 39 of 2004).
[12] Zheng LG, Zhou H, Cen KF, Wang CL. A comparative study of optimization algorithms for low NOx combustion modification at a coal-fired utility boiler. Expert Syst Appl 2009;36:2780–93.
[13] Ma L, Fang Q, Yin C, Wang H, Zhang C, Chen G. A novel corner-fired boiler system of improved efficiency and coal flexibility and reduced NOx emissions. Appl Energy 2019;238:453–65.
[14] Li S, Xu T, Hui S, Wei X. NOx emission and thermal efficiency of a 300MWe utility boiler retrofitted by air staging. Appl Energy 2009;86:1797–803.
[15] Zhou H, Zhao JP, Zheng LG, Wang CL, Cen KF. Modeling NOx emissions from coal-fired utility boilers using support vector regression with ant colony optimization. Eng Appl Artif Intell 2012;25:147–58.
[16] Li Q, Yao G. Improved coal combustion optimization model based on load balance and coal qualities. Energy 2017;132:204–12.
[17] Chen H, Liang Z. Damper opening optimization and performance of a co-firing boiler in a 300 MWe plant. Appl Therm Eng 2017;123:865–73.
[18] Bălănescu DT, Homutescu VM. Experimental investigation on performance of a condensing boiler and economic evaluation in real operating conditions. Appl Therm Eng 2018;143:48–58.
[19] ISO 12902. Solid mineral fuels – determination of total carbon, hydrogen and nitrogen – instrumental methods. 2001.
[20] ASTM D4239 – 14: Standard Test Method for Sulphur in the Analysis Sample of Coal using High-Temperature Tube Furnace Combustion.
[21] ISO 1928. Determination of gross calorific value by the bomb calorimetric method and calculation of net calorific value. 2009.
[22] ISO 1171. Solid mineral fuels D determination of ash. 2010.
[23] ISO 7404-3. Methods for the petrographic analysis of bituminous coal and anthracited Part 3: method of determining maceral group composition. 1994.
[24] ISO 7404-5. Methods for the petrographic analysis of bituminous coal and anthracited Part 5: method of determining microscopically the reflectance of vitrinite. 1994.
[25] ASTM D3682 – 13: Standard Test Method for Major and Minor Elements in Combustion Residues from Coal Utilization Processes.
[26] Van Niekerk D, Mitchell GD, Mathews JP. Petrographic and reflectance analysis of solvent-swelled and solvent-extracted South African vitrinite-rich and inertinite-rich coals. Int J Coal Geol 2010;81:45–52.
[27] Wagner N, Eble C, Hower J, Falcon R. Petrology and palynology of select coal samples from the Permian Waterberg Coalfield, South Africa. Int J Coal Geol 2019;204:85–101.
[28] Moroeng OM, Wagner NJ, Brand DJ, Roberts RJ. A nuclear magnetic resonance study: implications for coal formation in the witbank coalfield, South Africa. Int J Coal Geol 2018;188:145–55.
[29] Cloke M, Lester E, Thompson AW. Combustion characteristics of coals using a drop-tube furnace. Fuel 2002;81:727–35.
[30] Faure K, Willis JP, Dreyer JC. The grootegeluk formation in the Waterberg Coalfield, South Africa: facies, palaeoenvironment and thermal history — evidence from organic and clastic matter. Int J Coal Geol 1996;29:147–86.
[31] Guo L, Zhai M, Wang Z, Zhang Y, Dong P. Comprehensive coal quality index for evaluation of coal agglomeration characteristics. Fuel 2018;231:379–86.
[32] O'Keefe JMK, Bechtel A, Christanis K, Dai S, DiMichele WA, Eble CF, Esterle JS, Mastalerz M, Raymond AL, Valentim BV, Wagner NJ, Ward CR, Hower JC. On the fundamental difference between coal rank and coal type. Int J Coal Geol 2013;118:58–87.
[33] Park HY, Lee JE, Kim HH, Park S, Baek SH, Ye I, Ryu C. Thermal resistance by slagging and its relationship with ash properties for six coal blends in a commercial coal-fired boiler. Fuel 2019;235:1377–86.
[34] Hancox PJ, Götz AE. South Africa's coalfields—a 2014 perspective. Int J Coal Geol 2014;132:170–254.
[35] Phiri Z, Everson RC, Neomagus HWJP, Wood BJ. The effect of acid demineralising bituminous coals and de-ashing the respective chars on nitrogen functional forms. J Anal Appl Pyrol 2017;125:127–35.
[36] Qi M, Luo H, Wei P, Fu Z. Estimation of low calorific value of blended coals based on support vector regression and sensitivity analysis in coal-fired power plants. Fuel 2019;236:1400–7.
[37] Santhosh Raaj S, Arumugam S, Muthukrishnan M, Krishnamoorthy S, Anantharaman N. Characterization of coal blends for effective utilization in thermal power plants. Appl Therm Eng 2016;102:9–16.
[38] Vuthaluru HB, Brooke RJ, Zhang DK, Yan HM. Effects of moisture and coal blending on Hardgrove grindability index of western Australian coal. Fuel Process Technol 2003;81:67–76.
[39] Yusuff AS, Bhonsle AK, Trivedi J, Bangwal DP, Singh LP, Atray N. Synthesis and characterization of coal fly ash supported zinc oxide catalyst for biodiesel production using used cooking oil as feed. Renew Energy 2021;170:302–31.
[40] Wagner NJ, Tlotleng MT. Distribution of selected trace elements in density fractionated Waterberg coals from South Africa. Int J Coal Geol 2012;94:225–37.
[41] Moron W, Rybak W. NOx and SO_2 emissions of coals, biomass and their blends under different oxy-fuel atmospheres. Atmos Environ 2015;116:65–71.
[42] Verma VK, Bram S, Delattin F, De Ruyck J. Real life performance of domestic pellet boiler technologies as a function of operational loads: a case study of Belgium. Appl Energy 2013;101:357–62.
[43] Krzywanski J, Czakiert T, Shimizu T, Majchrzak-Kuceba I, Shimazaki Y, Zylka A, Grabowska K, Sosnowski M. NOx emissions from regenerator of calcium looping process. Energy Fuels 2018;32:6355–62.
[44] Li S, Xu Y, Gao Q. Measurements and modelling of oxy-fuel coal combustion. Proc Combust Inst 2019;37:2643–61.
[45] de Diego LF, Londono CA, Wang XS, Gibbs BM. Influence of operating parameters on NOx and N2O axial profiles in a circulating fluidized bed combustor. Fuel 1996;75:971–8.
[46] Ti S, Kuang M, Wang H, Xu G, Niu C, Liu Y. Experimental combustion characteristics and NOx emissions at 50% of the full load for a 600-MWe utility boiler: effects of the coal feed rate for various mills. Energy 2020;196:117128.
[47] Jiang Y, Lee BH, Oh DH, Jeon CH. Influence of various air-staging on combustion and NOX emission characteristics in a tangentially fired boiler under the 50% load condition. Energy 2022;244:123167.
[48] Mendes N, Bazzo LJ, Azevedo JT. Thermal conductivity analysis of an ash deposit on boiler superheater. Powder Technol 2017;318:329–36.